

Application of a Cloud Model to Cooling Tower Plumes and Clouds

HAROLD D. ORVILLE, JOHN H. HIRSCH AND LAURENCE E. MAY¹

Institute of Atmospheric Sciences, South Dakota School of Mines and Technology, Rapid City, 57701

(Manuscript received 10 October 1979, in final form 8 June 1980)

ABSTRACT

A steady-state, one-dimensional cloud model has been modified to simulate the growth of plumes (both wet and dry) and clouds from natural and forced draft cooling towers. The modifications to the cloud model are discussed and comparisons are made between predicted height and length of plumes and observed values. A correlation coefficient of 0.78 is achieved for model predictions of plume height and a correlation coefficient of 0.49 for predicted plume length. Comparisons with Benning Road data showed 78% of the model-predicted plume heights were within 50% of the observed height, while 93% of the predicted plume lengths were within 50% of the observed length.

Analysis of the model predicted plumes for a year's morning and evening atmospheric soundings is presented. Comparison of plumes during winter and summer showed dramatic changes, with the longest plumes occurring during the winter. Summer plumes were much shorter with relatively small visible plume heights and tall dry extensions above the visible plume.

A case of wet plume/dry plume/cloud formation is presented to illustrate output from the model.

1. Introduction

Numerical cloud models have been applied to cooling tower emissions for the past few years (Hanna, 1976; Lee, 1977; Hane, 1978; Murray *et al.*, 1978). The steady-state models are relatively simple and can be run on many soundings to produce a cloud climatology (Weinstein, 1972). The field-of-motion models as used by Murray and Hane are more realistic but require much more computer time and hence are used on case studies. As cooling towers become more prevalent, the application of the cloud models to various power plant configurations becomes attractive. Early plume models were concerned with smaller sources and sometimes neglected condensation (Slawson and Csanady, 1971).

The purpose of this paper is to describe briefly the application of a widely used cloud model to cooling-tower plume emissions from both natural and mechanical draft towers. The model is a steady-state, one-dimensional numerical cloud model developed by Hirsch (1971)² and associates. It is a revision of a steady-state cloud model developed by Weinstein and Davis (1968).³ The model was used

extensively during Project Cloud Catcher, conducted by the Institute of Atmospheric Sciences at Rapid City, South Dakota (Dennis *et al.*, 1974).⁴ Use of this model included the simulation of growth of cumuli in the Great Plains region and the evaluation of the seedability of clouds and the production of hail during cloud growth. The model uses the cloud microphysics of Wisner *et al.* (1972) and the entrainment concepts of Stommel (1951). For a complete description of the model, see Hirsch (1971).²

A similar cloud model has been applied to wet plumes by Hanna (1976). Considerations were given to the concept of bent-over plumes and the reduction of buoyancy and increase in mixing rates compared to vertical plumes (Briggs, 1975). A factor E_m of 2.25, "the ratio of the effective momentum flux to the momentum flux within the temperature plume" and a factor E_w of 0.5, "the ratio of the cross-sectional area of the moisture plume to the temperature plume" were used in the temperature and momentum equations. Lee (1977) developed a steady-state model for plume and clouds without using the E_m , E_w factors of Hanna and obtained equally good results as Hanna when applied to data from the Amos plant.

We do not use these factors in our cloud model but obtain results with comparable correlations between plume heights and lengths, although com-

¹ Present affiliation: Health Physicist, E. I. Dupont, Aiken, SC 29801.

² Hirsch, J. H., 1971: Computer modeling of cumulus clouds during Project Cloud Catcher. Rep. 71-7, Institute of Atmospheric Sciences, S.D. School of Mines and Technology, 61 pp.

³ Weinstein, A. I., and L. G. Davis, 1968: A parameterized numerical model of cumulus convection. Rep. 11, Pennsylvania State University, 44 pp.

⁴ Dennis, A. S., A. Koscielski, J. H. Hirsch, D. E. Cain and P. L. Smith, Jr., 1974: Cloud Cather report for 1972. Rep. 74-4, Institute of Atmospheric Sciences, S.D. School of Mines and Technology, 121 pp.

parison with the same data base has not been done by us. The increase in mixing coefficient we ascribe for the plume portion of the integration (described below) may have empirically incorporated many of the effects of mixing in bent-over plumes. In addition, we use a completely different method than Hanna for predicting horizontal displacement of the plume to obtain plume length. Finally, the model simulates both dry and wet plume rise and cloud growth; all three modes are possible with a single sounding. The model has been tested by the Argonne Laboratory Atmospheric Science Group and found to give results comparable to the better plume models (Policastro and Carhart, 1979).⁵

a. Method of approach

Several modifications were made to the steady-state cloud model to enable it to simulate the plumes produced by both natural and forced draft cooling towers. Changes were made to the height step, entrainment parameter, and initial liquid water content. The modifications to the model were tested against data taken from a study by Meyer (1974)⁶ of cooling tower plumes at the Potomac Electric Benning Road Power Plant in Washington, DC.

Input data needed for the model include the initial radius of the plume updraft (tower exit radius), the initial updraft velocity of the effluent, the effluent temperature and an atmospheric sounding. For model calibration, these data were obtained from measurements taken at the top of one of the mechanical draft cooling towers and from upper air soundings of the atmosphere taken at the time and in the vicinity of the observations. The initial updraft radius was taken as if the eight-cell or seven-cell cooling towers in operation at the time acted as one; i.e., the equivalent radius equals \sqrt{n} times a single radius, where n is the number of towers active. The sources are combined immediately, not delayed until the radius of the plume is equal to one-half the distance between towers, as in Hanna (1976) or Lee (1977). No provision was made for the wind direction to be either along or perpendicular to the line of towers. These multiple source effects and wind effects are thus submerged in the calibration technique.

Various parameters were then tested separately to determine their effect on the model. Once all tests were completed, the best combination of height step, mixing, etc., was used to calibrate the model against the Benning Road data. Results of these tests

and the comparison of the simulated plumes to the observed are discussed in Section 2b.

The model was then run using morning and evening rawinsonde data from Flint, Michigan, for three different cooling tower configurations. The three cooling tower configurations were a mechanical draft cooling tower using fossil fuel (600 MWe),⁷ a mechanical draft tower for a nuclear power station (2300 MWe), and a natural draft cooling tower for a nuclear power station (2300 MWe). Tower characteristics were supplied by Donald J. Portman and are given in Appendix B. Plume growth and downwind dispersion are then compared for each of the three cooling tower configurations.

Finally, a case is presented which shows the output of the model when a dry plume portion intercedes between wet plume and cloud formation.

2. The model

a. Original cloud model

The model used in this study is a modified version of the Institute of Atmospheric Sciences' (IAS) steady-state one-dimensional cloud model (Hirsch, 1971).² The original model predicts the maximum growth of cumulus convection using initial conditions at cloud base and an atmospheric sounding. The parcel method is used with moist-adiabatic ascent and mixing being calculated separately at each height step. An atmospheric sounding is interpolated at 200 m height intervals. An entrainment parameter of $2\alpha = 0.15$ is used throughout the entire cloud growth. Horizontal displacement of the cloud is based on the horizontal wind speed and the average speed of the updraft in the height interval.

Major limitations of this model are as follows:

- 1) The model predicts maximum growth only of the cloud under given initial conditions at cloud base and in the environment.
- 2) The model does not treat the cloud dissipation stage.
- 3) The model neglects horizontal asymmetries.
- 4) The model lacks a realistic scheme for the prediction of fallout of precipitation.

Some of the advantages of the model include the small computer storage needed to run the model and the short program execution time necessary to give the vertical profiles of cloud parameters. The model has proven to be a very useful tool in the analysis of seedability of clouds, as demonstrated during Project Cloud Catcher (Hirsch, 1971).² The various options available in the model permit flexibility in its use as a research tool. A variable updraft radius or a constant updraft radius can be used. Water

⁵ Policastro, A. J., R. A. Carhart, S. Ziemer and K. Haake, 1979: Evaluation of mathematical models for single and multiple source natural-draft cooling tower plume dispersion. Argonne National Laboratory, 493 pp.

⁶ Meyer, J. H., 1974: Mechanical draft cooling tower visible plume measurement program for plume modeling. The Johns Hopkins University Applied Physics Laboratory.

⁷ MWe denotes megawatts of electrical power.

loading of the updraft is available and an adjustment to the vertical velocity based on the shear of the horizontal wind can be selected. Freezing of cloud water can be either instantaneous; i.e., at one level or a function of temperature according to an exponential relationship.

The basic thermodynamic and dynamic equations

$$\frac{dT}{dz} = \frac{-g \left(1 + \frac{qL_e}{RT} \right) - \mu(T - T_e) - \frac{\mu L_e}{C_p} (q - q_e)}{1 + \frac{\epsilon L_e^2 q}{C_p R T^2}} \quad (1)$$

The first term on the right represents the moist-adiabatic temperature decrease of the parcel as it rises through the height step Δz . The second term is used to determine the heat loss due to entrainment of cool dry air from the environment. The last term also contributes to the temperature decrease as heat is lost through evaporation in order to maintain saturation of the parcel after mixing.

Conservation of water is obtained from a mass continuity equation:

$$\frac{dQ}{dz} = \frac{dQ_c}{dz} + \frac{dQ_i}{dz} + \frac{dQ_h}{dz} + \frac{dQ_g}{dz} = - \frac{dQ_s}{dz} \quad (2)$$

The total water dQ is distributed between cloud water, cloud ice, rainwater and precipitating ice (graupel and hail). Expansion of each of the terms on the right side of the equation shows the production of each form of water and its distribution through means such as condensation, freezing, accretion or autoconversion. Precipitation fallout is not included in the continuity equation here, but is permitted as an option. The precipitation fallout scheme used in the model is that of Simpson and Wiggert (1969). It is applied to the last two terms in (2) for rainwater and graupel.

Entrainment is expressed as a function of the radius of the updraft where

$$\mu = \frac{1}{M} \frac{dM}{dz} = \frac{2\alpha}{R} \quad (3)$$

The dynamics of the model use a conservation equation for vertical momentum to find the velocity of the updraft. Parcel acceleration is based on the buoyancy determined from the virtual temperature excess over the ambient air. This acceleration is decreased by the drag due to the weight of the water and the loss due to entrainment of the environmental air. The equation of motion for vertical velocity is given by

$$\frac{1}{2} \frac{dw^2}{dz} = g \left(\frac{T_v - T_{ve}}{T_{ve}} - Q \right) - \mu w^2 \quad (4)$$

used in this model will be given here. A complete review of the microphysics of the model can be obtained from Hirsch (1971)² and Wisner *et al.* (1972). A listing of the symbols used in the equations may be found in Appendix A.

The first law of thermodynamics (1) is used to express the change in cloud temperature with height:

In finite-difference form the equation becomes

$$w_1 = \left[(1 - 2\mu\Delta z) w_0^2 + 2g\Delta z \left(\frac{T_{v1} - T_{ve1}}{T_{ve1}} - Q_1 \right) \right]^{0.5} \quad (5)$$

An adjustment to the velocity of the updraft for the shear of the horizontal wind is permitted in the model (Malkus, 1952). The shear correction is given by

$$U_1 = \frac{U_0 + \mu\Delta z U_{e1}}{1 + \mu\Delta z} \quad (6)$$

$$w_1' = [w_1^2 - (U_1 - U_{e0})^2]^{0.5} \quad (7)$$

This adjustment is normally used in the cloud model, but is not permitted during the time of initial plume growth. Tests with the model indicate best results when the adjustment for the wind shear is turned on at 400 m above the height of the stack. The wind shear adjustment will be discussed in more detail in Section 3a.

b. Cooling tower plume model

1) PLUME HEIGHT

In order to adapt the cloud model just described to the calculation of plumes from cooling towers, several modifications were made to the cloud model to better simulate the smaller scale phenomenon. There were four major changes to the model: 1) the reduction of the height step from 200 m to 2 m at tower top; 2) the specification of an entrainment parameter 2α of 0.3; 3) the arbitrary specification of an initial liquid water content of 0.001 g g^{-1} at tower top to simulate the wet effluents; and 4) the modification of the model to predict dry as well as wet plume rise (i.e., dry adiabatic ascent as well as moist adiabatic ascent with mixing and loading).

A unique modification of the model is that as the size of the plume grows, the model reverts back to

the calculations more in line with larger plumes, and finally that of cumulus. An example of this is the height step. The height step (Δz) used in the calculations was set at 2 m for the region immediately above the tower. After the plume reaches a height of 400 m above the ground, a transition begins to increase the height step exponentially to a 200 m interval at 2500 m above the ground. This gradual transition interval was chosen because of the sensitivity of the model to rapid changes in Δz , and the average cloud base for most areas within the United States. No attempt was made to distinguish between a cloud and a plume in the transition zone, except to assume that once the 2500 m height is reached, cumulus cloud characteristics are assumed.

The entrainment parameter for the model is also changed in the same manner as the height step. The only difference is that the transition zone is based on the stack height instead of height above the ground, since three different tower configurations were run at the same time using different stack heights. The entrainment parameter 2α was set at 0.3 for the first 400 m of plume growth and reduced exponentially to 0.15 at the 2500 m level. Both of these values are determined empirically, the 0.3 from the Benning Road data and the 0.15 from radar and cloud data in this region.

The variable cloud radius option of the cloud model was used throughout this study. The sensitivity analysis from the original cloud model showed that a variable cloud radius produced a 1.6% smaller cloud-top height and a 4.4% lower maximum vertical velocity than with a constant radius cloud. Since the updraft radius of the moist plume produced by cooling towers is much smaller (from 0.01 km for a mechanical draft cooling tower to 0.0474 km for a natural draft cooling tower) than that for cumulus development (from 0.5 km or larger), the entrainment rate as given by (3) would be much too high for the upper portions of the cloud. The updraft radius is derived from (3) and the definition of mass flux in a one-dimensional cloud model ($M \equiv \pi R w \rho$), and is given by

$$R_1' = R_0' \left[\frac{\rho_0 w_0}{\rho_1 w_1} \exp\left(\frac{2\alpha}{R_0'} \Delta z\right) \right]^{0.5} \quad (8)$$

The variable cloud radius permits the growth of the radius of the plume with height and the corresponding decrease in the entrainment rate with the growth as would be expected from a concentrated source such as a cooling tower.

Water loading in the updraft is permitted throughout the plume and cloud growth. The water loading option reduces the vertical velocity of the updraft by the weight of the liquid water carried aloft by the updraft.

The plume height is taken as that height where the vertical velocity goes to zero.

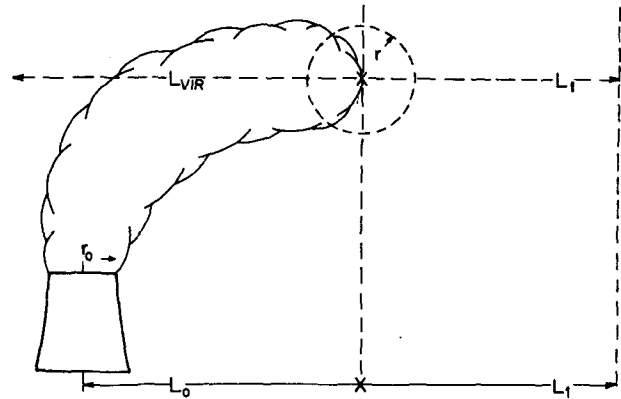


FIG. 1. Plume diagram.

2) PLUME LENGTH

The total plume length is calculated in two parts: one part is the horizontal displacement during the vertical rise of the plume; the second is dispersion downwind after the rise has ceased. The two displacements are then added to obtain the total plume length. Horizontal displacement of the plume during its vertical rise is simply a number of U times t calculations, where U is the speed of the horizontal wind at the top of the grid interval and t the time available for displacement in each height interval; i.e., $\Delta t/\bar{w}$ where \bar{w} is the mean vertical velocity in the interval Δz .

An individual component of the displacement is given by

$$\Delta L = \frac{\Delta z U}{\bar{w}_1} \text{ [m]} \quad (9)$$

All ΔL 's are summed to give L_0 , as shown in Fig. 1. This displacement is then added to the dispersion of the plume downwind using the Gaussian dispersion model from Turner (1969) to obtain the total plume length and is described next (also, see Eagles and Kohlenstein, 1974).⁸ This technique models horizontal eddy mixing of the plume in the downwind direction.

The dispersion technique is applied at the top of the visible plume which is defined as the lowest height at which a liquid water content of less than 0.001 g kg^{-1} occurs, or the level at which the vertical velocity goes to zero. The excess water vapor mixing ratio over that of the environment and the liquid water in the plume at the cloud top constitute the source term in the Gaussian plume model. Calculations of σ_y , σ_z , the standard deviations of the concentration distribution, are calculated using the cloud

⁸ Eagles, T. W., and L. C. Kohlenstein, 1974: A cooling tower visible plume prediction model based on measurements. Presented at 55th Annual Meeting of the American Geophysical Union, Washington, D.C.

TABLE 1. Single unit characteristics of PEPCO's Benning Road power generating and cooling tower units 15 and 16.

Power generation capacity	289 MWe
Normal full load operation	280 MWe
Circulating water flow	8190 L s ⁻¹
Approximate physical dimensions of cooling tower:	
Length	90 m
Width	18 m
Height	18 m
Number of cooling cells	8
Fan size	8.4 m
Fan motor size	112 kW
Diameter of cell opening at top	9.3 m
Average wake-up water under full load	151.2 L s ⁻¹
Average blow down	18.9 L s ⁻¹
Temperature range across condensers	13.3°C
Cooling tower construction—wood, fiberglass and asbestos	
Cooling tower manufacturer	Marley

plume as a virtual area source. The two criteria (cloud water and vertical velocity) are needed to assure that some water (excess vapor or liquid) is available to be dispersed downwind.

The downwind dispersion L of the plume is defined as a function of the product of the standard deviations as given by

$$L = 10^{\{(\log_{10}(\sigma_y\sigma_z) - 4.23)/1.89\}} \text{ [km]}, \quad (10)$$

where the constants 4.23 and 1.89 have been determined from the Class B stability of Turner (1969). To insure that the source strength for the dispersion of the plume does not increase initially downwind from L_0 , the virtual distance L_{VIR} (Fig. 1) was calculated using (10) with the assumption that

$$\sigma_y\sigma_z = (r_0S)^2 = R'^2 \text{ [m}^2\text{]}, \quad (11)$$

where r_0 is the initial plume radius at tower exit, and S the ratio of the actual radius R' to the initial radius [R' is given by (8)]; note that R' is denoted by the symbol r in Fig. 1]. See Turner (1969, pp. 39 and 55) for a discussion of the virtual distance.

The solution for the horizontal dispersion L_1 after vertical wet plume rise had ceased was found using

$$\sigma_y\sigma_z = \frac{\chi_0 R'^2}{q_{se} - q_e} \text{ [m}^2\text{]} \quad (12)$$

in (10) where χ_0 is the excess water substance (vapor plus cloud liquid mixing ratios) at the distance L_0 , q_{se} is the saturation mixing ratio of the environment, and q_e the environmental water vapor mixing ratio. Using the solution of (12) in (10) gives the downwind distance $L_{\text{VIR}} + L_1$. The plume length L_1 due only to the downwind dispersion is found by subtracting the distance L_{VIR} from $L_{\text{VIR}} + L_1$. The total horizontal displacement of the plume is given by adding L_0 to L_1 .

3. Results and discussion

a. Benning Road data comparison

The initial tests of the model were done with a constant entrainment parameter and height step. Calibration of the model was accomplished using the Benning Road Power Station data (Table 1) which has a maximum height of a visible plume of 360 m MSL. This puts the height of all observed plumes used in the Benning Road analysis below the height for which any parameter begins to change exponentially. Twenty-seven of the 48 cases provided data for the calibration test. The Argonne Laboratory tests have used the model on more general data.

Running the model using a large height step produced unsaturated plumes above the cooling tower with the saturated plume appearing only after several height steps. Similar results were obtained in a report from EG&G, Inc. (1970).⁹ Their study used 200 m height steps and a small entrainment parameter for the entire plume growth which produced unsaturated plumes for several height steps above the stack, which is not in agreement with observations. Smaller height steps produce saturated plumes at the top of the tower. A height step (Δz) of 2 m was found to give the best results. Height steps of 5, 2 and 1 m were tested. Table 2 shows the effect of using different height steps, and the percent difference from the observed values. Standard deviations are given to show the variation of the plumes.

The smaller height steps produced much larger plume heights. In general, a $\Delta z = 5$ underpredicted the smaller heights and overpredicted the larger heights. This is also true of the model in its present form (with $\Delta z = 2$ m at tower top), although the degree of error is much less, as shown in Fig. 2. The average value of plume height and standard deviation for $\Delta z = 5$ m are closer to observations in Table 2 than for a $\Delta z = 2$ m, but the number of predictions within 50% of the observed values were much less.

The model was run on a CDC 3400 computer at the School of Mines and Technology in Rapid City, South Dakota. Processing time for the Benning Road data was ~ 14 min for a height step of 2 m. This compares to a time of 9 min for $\Delta z = 5$ m and 23 min for 1 m height steps. Computation time (cost) was not a factor in tuning of the model, but it is worth noting the considerable savings by using larger intervals for dz for calculations.

A liquid water content of 0.001 g g^{-1} was assumed as the plume leaves the cooling tower. The addition of liquid water in the plume which is assumed to be

⁹ EG&G, Inc., 1970: Potential environmental modifications produced by large evaporative cooling towers. Final Report, Contract 14-12-542, Federal Water Pollution Admin., Boulder, CO.

TABLE 2. Average height of plumes (m) using different height steps (m). $2\alpha = 0.3$; $Q_0 = 0.001 \text{ g g}^{-1}$. Numbers in parentheses are percent differences from the observed.

dz (m)	1	2	5	Obs
Average height	192 (+15)	189 (+13)	152 (-7)	164
Standard deviation	102 (+29)	97 (+25)	90 (+20)	72

TABLE 3. Average height of plumes (m) using different height steps (m). $2\alpha = 0.3$; $Q_0 = 0.0005 \text{ g g}^{-1}$. Numbers in parentheses are the percent difference from the observed.

dz (m)	1	2	5	Obs
Average height	182 (+9)	179 (+8)	135 (-18)	164
Standard deviation	102 (+29)	98 (+27)	94 (+23)	72

saturated when it leaves the tower causes a higher plume growth, as can be seen from comparing Table 3 with Table 2. Presumably, the slight increase in drag (loading of the updraft) is overcompensated by the extra water available to maintain the plume to a greater height.

Table 3 shows the effect of reducing the initial liquid water content from 0.001 g g^{-1} as in Table 2 to 0.0005 g g^{-1} . Plume heights were lower in all cases except where there was no dry plume growth. Most days had a moist plume with a dry portion extending above the plume. When cloud water remained with the vertical velocity going to zero at the top of the plume, the heights were the same with more cloud water remaining at the top when using the greater initial liquid water content. The change made about a 5% decrease in heights overall, with the largest effect on plumes less than 200 m. The overall effect of the liquid water content is not nearly as large as the effect of the height step or the entrainment parameter.

The cloud width varies in direct proportion to its height, which affects the entrainment rate because of the decreased surface-to-volume ratio of the plume. This variation of entrainment was most apparent in

the smaller plumes. A change of $2\alpha = 0.3-0.4$ resulted in 50% smaller plumes for cases where the plume height was less than 150 m, while larger plumes had only a 20% reduction in height. As shown in Table 4, the average heights of the plumes drop drastically with a small increase in the entrainment parameter.

An entrainment parameter of $2\alpha = 0.3$ was used for the first 400 m of plume growth. The entrainment rate changed rapidly during the initial growth as the radius of the updraft expanded from the relatively small cooling tower radius. For example, the increase in radius during 100 m vertical growth for the 31 October sounding showed an increase from 13 m to 30 m. This represents a reduction in the entrainment rate from 0.032 to 0.01 m^{-1} .

The model parameters were chosen based on the height predictions alone. The plume length was then tested using the same parameters, which were found to give the best plume length predictions also. There were several other factors which had a significant effect on the plume length. These were the horizontal wind shear and the stability class from Turner (1969).

The horizontal wind shear has an indirect effect as it is applied through an adjustment to the vertical velocity, as given by (6) and (7). Most cases of the Benning Road data had little or no wind speed shear during the growth of the plume. When there was large wind shear, the plume length became several times longer than the observed. The component of plume length that is a result of the displacement of the plume during growth as given by (9) is dependent upon the mean vertical velocity \bar{w}_1 for the height interval Δz . Strong wind shear produced small reductions in the vertical velocity and corresponding increases in the horizontal displacement. The cumula-

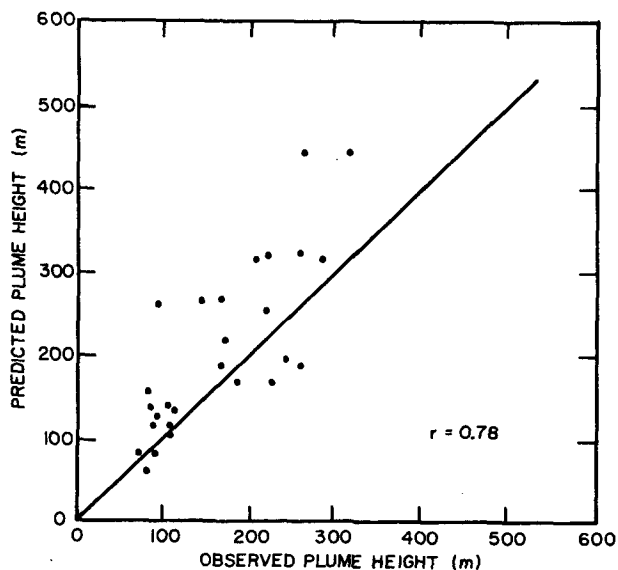


FIG. 2. Model-predicted vs observed plume height— $\Delta z = 2 \text{ m}$.

TABLE 4. Average height (m) of plumes using different entrainment parameters. $dz = 5 \text{ m}$; $Q_0 = 0.001$. Numbers in parentheses are the percent difference from the observed.

2α	0.3	0.4	0.6	Obs
Average height	152 (-7)	99 (-40)	54 (-67)	164
Standard deviation	90 (+20)	71 (-1)	60 (-17)	72

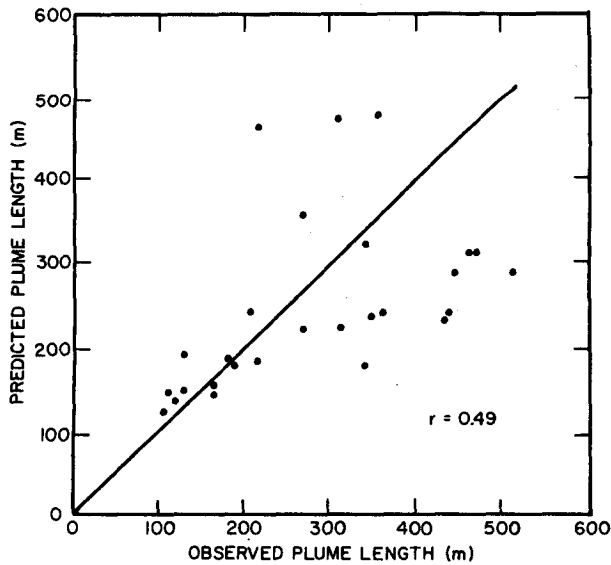


FIG. 3. Model-predicted vs observed plume length—Class B stability.

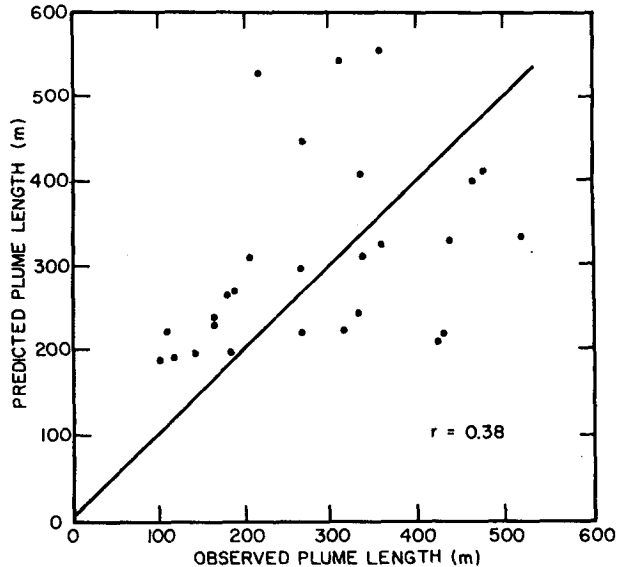


FIG. 5. Model-predicted vs observed plume length—Class C stability.

tive effect was quite large for plume heights of 200 m or more. Eliminating the adjustment to the vertical velocity during initial plume growth caused less than a 1% additional plume rise and eliminated the problem with the plume length. Above 400 m, the wind shear adjustment can be used.

The model uses a Gaussian model from Turner (1969) to estimate the downwind dispersion of the visual plume after the vertical velocity goes to zero or the cloud water threshold is reached. Three stability classes were tested using the stability categories from Turner (1969). Class B stability was found

to give the best fit for the data as most cases fell into this category. A comparison of Fig. 3 with Figs. 4 and 5 show that the stability has a significant effect on the plume length. Class A stability plumes (the most unstable class) had a much smaller length, as shown in Table 5. This was expected since the standard deviations, σ_z , σ_y , for Class A stability are smaller as a result of lower surface wind speed and greater instability. As the wind speed increases, approaching Class C, the effluent from a continuous source is introduced into a greater volume of air per unit time interval, and the standard deviations increase giving a larger, more variable distribution of the data.

Figs. 2 and 3 show the relationship between the observed and predicted values of the plume height and length. A correlation coefficient of 0.78 for the predicted plume height and 0.49 for the plume length was obtained. While the correlation coefficients appear low, the percent of model predicted values within 50% of the observed value, as shown in Table 6, demonstrates that the model can be a useful indicator for the simulation of cooling tower plumes.

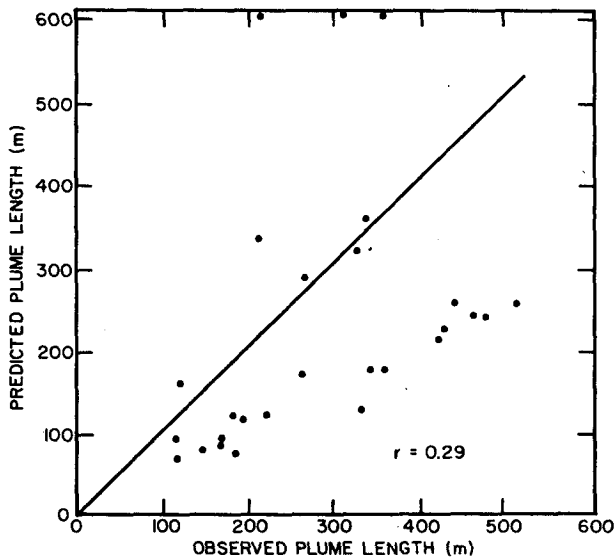


FIG. 4. Model-predicted vs observed plume length—Class A stability.

TABLE 5. Average length of plumes (m) using different class stability categories. Numbers in parentheses are the percent differences from the observed.

Class	A	B	C	Obs
Average length	231 (-18)	242 (-14)	310 (+9)	283
Standard deviation	170 (+28)	104 (-15)	109 (-11)	122

TABLE 6. Percent of cases where model predicted value was within the given percent of the observed value.

Percent error (%)	30	40	50
Height	67	70	78
Length	52	78	93

b. Flint, Michigan, climatology

The model was run using a year's (1972) data from Flint, Michigan, with a morning and evening sounding for each day. Three cooling tower configurations were tested in this study, a mechanical draft used at a conventional fossil fuel 600 MWe power plant, a mechanical draft tower, and a natural draft tower proposed for a 2300 MWe nuclear power plant. A more complete description of the tower configurations is given in Appendix B.

The model allows a dry adiabatic plus turbulent mixing rise of a dry plume when the vertical velocity is greater than zero and liquid water drops below the 0.001 g kg⁻¹ value. Heights of dry plumes include the visible plume heights. When there is no dry plume growth above the visible (wet) plume, the heights are equal.

The average height of the plumes for the entire year shows that the natural draft tower produces the largest plume with the peak for all towers occurring in May for both the morning and evening soundings. The mechanical draft cooling tower for the nuclear plant in all cases produces a higher plume than the conventional tower. This is expected since the towers are approximately the same height, but the flux is greater in the mechanical (nuclear) tower (3.76 × 10⁴ m³ s⁻¹ vs 2.13 × 10⁴ m³ s⁻¹).

In general, the largest plumes occur in the evening,

except for a few notable exceptions. January, which has no dry plume above the visible plume, had greater plume growth in the morning. The summer months also had higher plumes in the morning. During the colder, higher relative humidity winter months, there is no dry extension above the visible plume. Figs. 6 and 7 show the absence of dry plume growth during the months of November through February, with a few dry plumes occurring in March and October. The difference between the morning and evening plumes is the smallest during the winter, with only a slight increase in the difference between visible plumes in the summer. Although higher relative humidity occurs during the winter, increased stability explains the low plume heights.

Visible plume heights are slightly lower in summer than in winter, with a dry plume growth of several hundred meters. This is a result of the decreased relative humidity in the summer months. The separation between the wet and dry plumes is greatest in the evening as the stability decreases along with the relative humidity.

The first part of the summer, beginning with May and going through July, shows a larger visible plume in the morning, while the dry plume extension is greatest in the evening. By October, with the exception of the visible plume produced by the mechanical draft tower (conventional), the largest plumes occur in the evening and fewer plumes have a dry extension.

While the height of the plumes showed a direct relation to the type of cooling tower used, the length of the plume did not show a direct relation. The longest plumes occurred during the cold, stable winter months, with the natural draft tower producing the longest. The mechanical (600 MWe) draft tower produced the shortest plumes, except in September

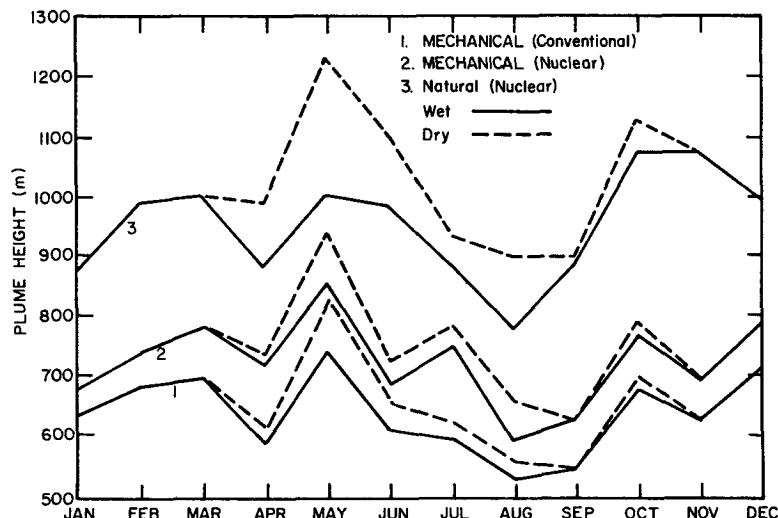


FIG. 6. Average plume height m (MSL)—morning.

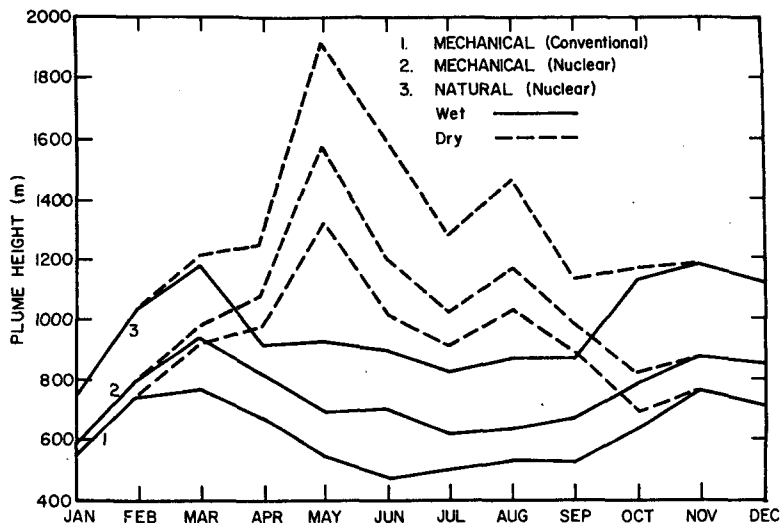


FIG. 7. Average plume height m (MSL)—evening.

during the morning. In general, the longest plumes occurred in the morning, with the summer showing the greatest difference between morning and evening. Plume lengths in the morning were as much as two to three times longer than in the evening during the summer, while winter produced plumes of more nearly the same size. Figs. 8 and 9 show the average plume length for the three cooling tower configurations. It can be seen that unlike the height, cooling tower configurations were not as important to the length, except in winter where larger tower configurations produced the longest plumes.

The winter months produced much longer plumes than summer with a greater variation between the plume lengths. Average plume lengths were distorted by a few very long plumes.

4. Cloud-triggering simulation

As power plants become larger, the potential for triggering clouds becomes greater. These clouds, in turn, could interact with other systems or develop further themselves to produce precipitation. A case is presented here that demonstrates the results of the steady-state cloud model regarding the forma-

tion of a plume-induced cumulus cloud and also shows the capability of the model to simulate dry as well as wet plume rise.

The case is well illustrated in Anthes *et al.* (1978) textbook regarding general meteorology. Plate 14 in the text illustrates a cumulus cloud growing over the Keystone power station.

Input data for the plume/cloud simulation is from the Large Power Plant Effluent Study (Schiermeier, 1970). A composite input sounding for the Keystone power plant was developed from the 1000 LT helicopter temperature profiles, the Jimmy Stewart Airport radiosonde run, and the pilot balloon measurement of winds aloft at the Keystone station on 1 May 1969. The temperature and moisture profiles are shown as solid lines on Fig. 10. Table 7 summarizes other initial conditions that were used in the Keystone power plant simulation. The graphical profiles shown in Fig. 11 depict the output from the steady-state numerical plume model. The visible plume grew to a height of ~700 m,¹⁰ where atmospheric conditions caused dry adiabatic ascent for another 167 m,

¹⁰ All heights are above ground level (AGL).

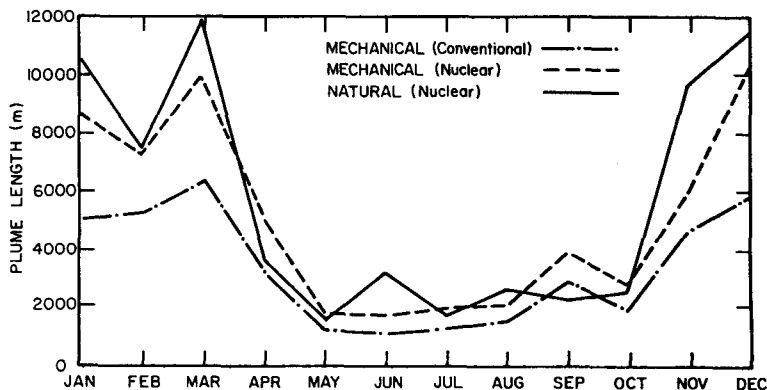


FIG. 8. Average plume length (m)—morning.

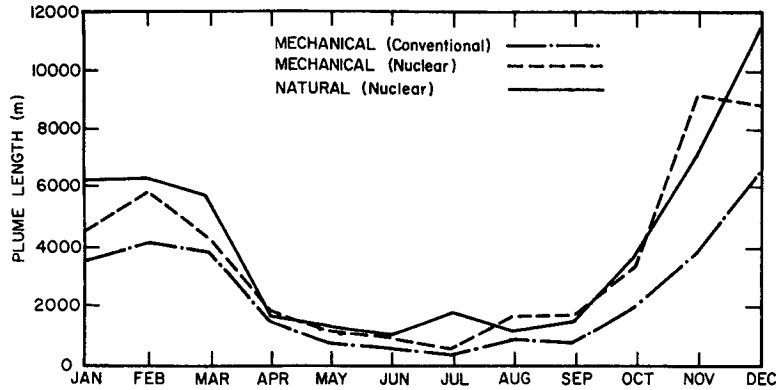


FIG. 9. Average plume length (m)—evening.

at which point a visible cloud formed and grew to a height of almost 200 m. The vertical velocity profile also shown in the figure increased during the plume phase to 11.6 m s^{-1} , decreased to 3.6 m s^{-1} , then increased again to over 9 m s^{-1} in the cloud region and decreased to zero at cloud top. The horizontal displacement of the plume downwind from the tower was $\sim 70 \text{ m}$, and the entire displacement of the cloud was over 780 m downwind from the plant.

The initial simulation from the steady-state plume/cloud model demonstrated the ability of the model to trigger initial cloud growth from a given set of initial conditions (atmospheric sounding and cooling tower effluents from the power plant).

The effluent study (Schiermeier, 1970) dealt primarily with data from the power plant stacks and offered very little in the way of verification data from the cooling towers. An examination of the photograph (Anthes *et al.*, 1978) suggests that vertical dimensions of the plume should be on the order of 300–400 m, with a dry region extending to almost 1 km above the plume top and a cloud vertical development in excess of 1 km. Adjustments were made in the atmospheric sounding by decreasing the low-level moisture as shown by the dashed line in Fig. 10 in order to simulate more closely the photograph of the condensed plume and cloud. Fig. 12 shows the results from the numerical simulation. The plume depth is reduced to a height of 380 m, with a dry adiabatic region of $\sim 770 \text{ m}$ and a vertical cloud depth of 1275 m. The cloud was displaced 850 m downwind from the power plant. Table 8 summarizes the model output from the two Keystone simulations.

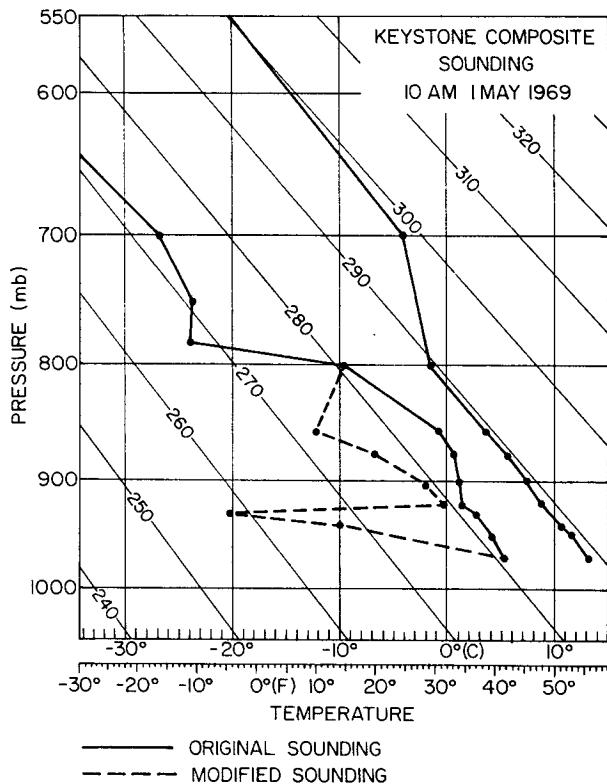


FIG. 10. Skew T diagram of 1 May 1969 atmospheric sounding.

5. Summary and conclusions

Description of the modifications made to a steady-state numerical cloud model to simulate the growth of plumes produced by natural and mechanical draft cooling towers is presented in this study. Modifications include reducing the height step from 200 m to 2 m, increasing the entrainment (2α) from 0.15 for clouds to 0.3, giving an initial liquid water content of 0.001 g g^{-1} to the plume at the top of the stack, and programming for dry as well as moist adiabatic ascent.

TABLE 7. Initial conditions for the Keystone power plant simulation.

Tower height	100 m AGL
Effective radius of towers (four towers – 32 m radius)	65 m
Effluent velocity at top of tower	10 m s^{-1}
Initial cloud water content at top of tower	0.1 g kg^{-1} *
Temperature of air at top of tower	12.5°C
Temperature of effluent at top of tower	32.0°C

* An amount $< 1.0 \text{ g kg}^{-1}$ was needed to give a dry plume section.

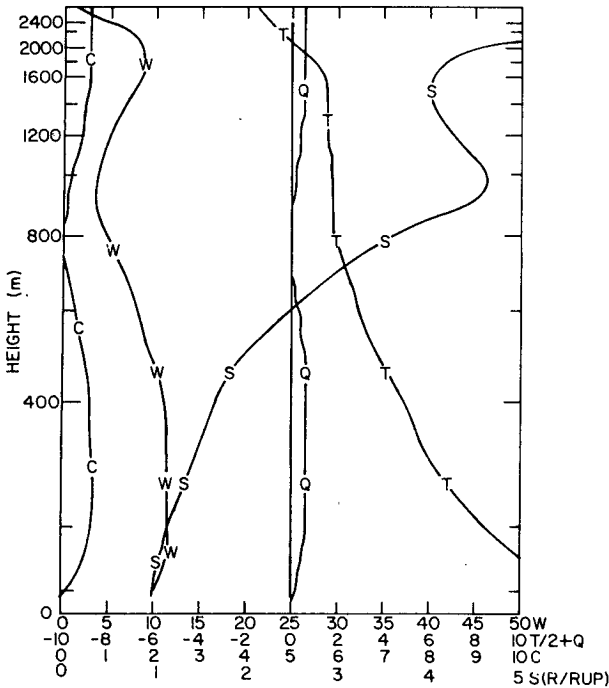


FIG. 11. Vertical plots of upward motion (W , $m\ s^{-1}$), buoyancy (T , $^{\circ}C$), total water content (Q , $g\ kg^{-1}$), cloud water content (C , $g\ kg^{-1}$) and radius ratio (S , updraft radius/initial radius) for the original sounding of 1 May 1969. Note the exponential change in vertical scale with height.

Plume length calculations are done in two steps. The horizontal displacement of the plume during vertical rise is based on the time of growth for each height step and the horizontal wind speed. A Gaussian model from Turner (1969) is used to estimate the

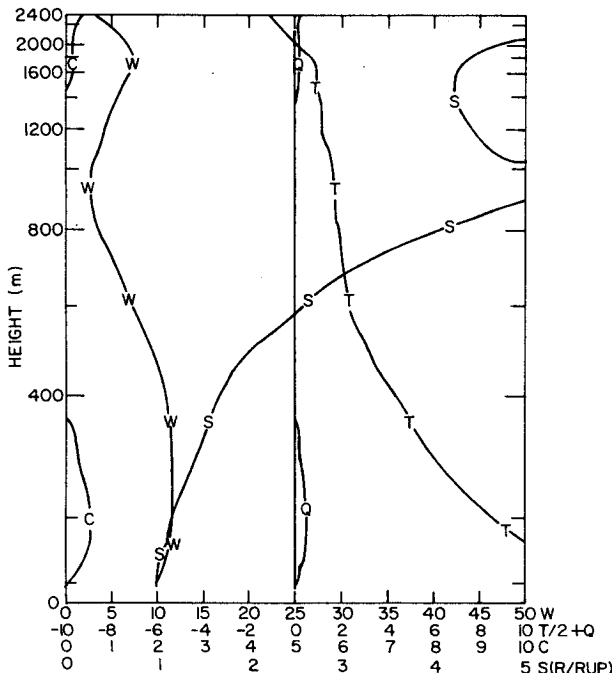


FIG. 12. As in Fig. 11 except for the modified sounding.

TABLE 8. Model output summary of Keystone simulation.

	Original sounding	Modified sounding
Plume height	706 m	380 m
Plume length	67 m	32 m
Dry depth	167 m	768 m
Cloud-top height	2588 m	2421 m
Downwind displacement	782 m	848 m

additional downwind dispersion of the visual plume after the vertical velocity goes to zero or the cloud water threshold is reached. Class B stability was found to give the best fit for the data.

When a plume reaches a height of 400 m above the top of the tower, the model exponentially changes the height step and entrainment parameter back to the values used for clouds. The transition is done between a height of 400 to 2500 m where the height step is fixed at 200 m and the entrainment parameter at $2\alpha = 0.15$.

The model was calibrated against data from the Johns Hopkins study of cooling tower plumes (Meyer, 1974). The correlation coefficient for model-predicted height versus observed height was 0.78, while the correlation coefficient for plume length was 0.49. The model generally underpredicts the heights of plumes with 78% of the predicted heights within 50% of the observations and overpredicts plume lengths with 93% of the plume lengths being within 50% of observed values.

Fall and winter soundings were used in the tuning of the model with no interaction of clouds or frontal systems being considered in this study.

The model was run using a year's (1972) data from Flint, Michigan, using three different cooling tower configurations as given in Appendix B. Morning and evening soundings for each day were used, with the natural draft cooling tower producing the largest plumes in all cases. Comparison of plumes during winter and summer showed dramatic changes, with the longest plumes occurring during the winter. Summer plumes were much shorter with relatively small visible plume heights and tall dry extensions above the visible plume.

Variation between plume heights from morning and evening was greatest during the summer, with evening producing the largest plume height.

A case of cloud triggering was run to illustrate the model output. A wet plume/dry plume/cloud situation from the Keystone power plant on 1 May 1969, illustrated in Anthes *et al.* (1978), was used for model input. The sounding needed to be modified in the moisture content in low levels to best simulate the actual situation. The failure can be attributed to the model mixing coefficient, other model weaknesses, atmospheric changes, or a combination of causes.

The model has shown that it can be a useful tool in the study of cooling towers and their effects on

the local environment. The need for further study is also demonstrated by the results of this model, which point out the variations of plume height and length with different cooling towers and different atmospheric conditions.

6. Suggestions for future research

This model has been calibrated against data from relatively cold soundings during the fall and winter. A study of plumes from cooling towers with soundings during the summer as well as winter is needed for tuning of models on a year-round basis. The interaction of the plumes with clouds and frontal systems has not been tested and could provide some useful information with respect to cloud triggering or possible enhancement. A more complete study of the possible environmental effects of cooling towers

using more advanced time-dependent models is needed as the release of larger amounts of waste heat into the atmosphere increases with the construction of more and larger power production facilities.

Acknowledgments. We appreciate greatly the advice and discussions with Professor Donald J. Portman of the University of Michigan.

This research was sponsored by the Atmospheric Sciences Section, National Science Foundation, under Grants ATM75-03882, ATM77-05187 and ATM-79-16147. The computations were done at the Computer Center of the South Dakota School of Mines and Technology.

Appreciation is extended to Mr. Melvin J. Flannagan for his skill in drafting the figures, and to Mrs. Joie Robinson for preparing the manuscript.

APPENDIX A

Symbols*

Symbol	Quantity	Value	Units
C_p	specific heat of air	1005	$\text{J kg}^{-1} \text{K}^{-1}$
g	acceleration of gravity	9.80	m s^{-2}
L_0, L_1	horizontal displacement		m or km
L_e	latent heat of condensation	2.5003×10^6	J kg^{-1}
M	mass flux		g s^{-1}
Q	total water (liquid + ice)		g g^{-1}
Q_c	cloud water content		g g^{-1}
Q_g	precipitating ice water content		g g^{-1}
Q_h	rainwater content		g g^{-1}
Q_i	cloud ice content		g g^{-1}
P	pressure		kpa
q	cloud mixing ratio		g g^{-1}
q_e	environment mixing ratio		g g^{-1}
q_{se}	environment saturation mixing ratio		g g^{-1}
R	gas constant for dry air	287.04	$\text{J kg}^{-1} \text{K}^{-1}$
R'	updraft radius		m
r_0	initial updraft radius		m
S	ratio r_0/R'		
T	temperature of cloud		K
T_e	temperature of environment		K
T_v	virtual temperature of cloud		K
T_{ve}	virtual temperature of environment		K
U	horizontal wind velocity		m s^{-1}
U_{e0}	horizontal wind velocity at cloud base		m s^{-1}
w	vertical velocity		m s^{-1}
Z	height		m
χ_0	concentration		g g^{-1}
Δz	height increment		m
σ_z	standard deviation in the vertical of the plume concentration distribution		m
σ_y	standard deviation in the crosswind direction of the plume concentration distribution		m
ϵ	molecular weight ratio	0.622	
μ	entrainment parameter	$2\alpha/R'$	m^{-1}

* Note: Subscripts 0 and 1 refer to previous and current height step values, respectively.

APPENDIX B

Cooling Tower Configurations

1. Mechanical draft cooling tower, conventional (fossil fuel) power station (600 MWe)

This station has four cooling towers of seven cells each, arranged in two rows (14 cells in each row). Each cell is 18 m (60 ft) high and 9 m (30 ft) in diameter. Stack top is at 254 m (833 ft) above mean sea level (MSL).

A worst possible situation is modeled—all 28 cell plumes are assumed to interact and rise as one, giving an equivalent radius of 24.2 m (79.4 ft). The initial exit vertical velocity is 11.6 m s^{-1} .

Effluent temperature T is given by:

$$T = 85 + (T_{WB}/5)^{\circ}\text{F} \quad \text{for } T_{WB} = -20 \text{ to } +30^{\circ}\text{F}$$

$$T = 79 + (T_{WB}/3)^{\circ}\text{F} \quad \text{for } T_{WB} = +30 \text{ to } +60^{\circ}\text{F}$$

$$T = 69 + (T_{WB}/2)^{\circ}\text{F} \quad \text{for } T_{WB} = +60 \text{ to } +80^{\circ}\text{F}$$

and T_{WB} is the environmental wet-bulb temperature in $^{\circ}\text{F}$.

2. Mechanical draft tower, nuclear power station (2300 MWe)

For this station there are four round units, 13 fans each, 77 m (73 ft) high, discharge area 72.2 m^2 (777.7 ft^2). The stack top is at 258 m (846 ft) MSL. Again, this assumes the worst possible case of all plumes (from 52 fans) joining after emission from tower top. An equivalent radius for this configuration is 34.6 m (113.5 ft).

The following equations were used for effluent temperatures:

$$T = 84 + (0.30T_{WB})^{\circ}\text{F} \quad \text{if } T_{WB} = 40^{\circ}\text{F}$$

$$T = 82 + (0.35T_{WB})^{\circ}\text{F} \quad \text{if } T_{WB} = 60^{\circ}\text{F}$$

$$T = 76 + (0.45T_{WB})^{\circ}\text{F} \quad \text{if } T_{WB} = 60^{\circ}\text{F}$$

The exit vertical velocity is 10.0 m sec^{-1} (22.4 mph).

3. Natural draft cooling tower, nuclear power station (2300 MWe)

This station has two hyperbolic towers, each 152 m (500 ft) high. Internal diameter of each at discharge is 67 m (220 ft). Stack top height is 388 m

(1273 ft) MSL, and the equivalent radius for the two towers together is 47.4 m (155.5 ft).

Effluent temperature is given by

$$T = 62.5 - T_{WB} \left[0.575 + \frac{(100 - \text{RH})}{1000} \right]^{\circ}\text{F},$$

where RH is relative humidity.

The exit velocity is given by

$$w_0 = 8.4 - T_{WB} \left[0.0317 + \frac{(100 - \text{RH})}{5000} \right] \text{ m s}^{-1}.$$

These temperatures, exit velocities and equivalent radius values are used for initial conditions in the numerical plume model.

REFERENCES

- Anthes, R. A., H. A. Panofsky, J. J. Cahir and A. Rango, 1978: *The Atmosphere*, 2nd ed. Merrill Publ. Co., 442 pp.
- Briggs, G. A., 1975: Plume rise predictions. *Lectures on Air Pollution and Environmental Impact Analyses*, Amer. Meteor. Soc., 59–111.
- Hane, C. E., 1978: The application of a two-dimensional convective cloud model to waste heat release from proposed nuclear energy centers. *Atmos. Environ.*, **12**, 1839–1848.
- Hanna, S. R., 1976: Predicted and observed cooling tower plume rise and visible plume length at the John E. Amos power plant. *Atmos. Environ.*, **10**, 1045–1052.
- Lee, Jjin-Lang, 1977: Potential weather modification from cooling tower effluents at conceptual power parks. *Atmos. Environ.*, **11**, 749–759.
- Malkus, J. S., 1952: Recent advances in the study of convective clouds and their interaction with the environment. *Tellus*, **4**, 71–87.
- Murray, F. W., L. R. Koenig and P. M. Tag, 1978: Numerical simulation of an industrial cumulus and comparison with observations. *J. Appl. Meteor.*, **17**, 655–668.
- Schiermeier, F. A., 1970: Large power plant effluent study [LAPPES]. Vol. 2, Instrumentation, procedures, and data tabulations [1967 and 1969]. National Air Pollution Control Admin., APTD 0589, 337 pp.
- Simpson, J. S., and V. Wiggert, 1969: Models of precipitating cumulus towers. *Mon. Wea. Rev.*, **97**, 471–487.
- Slawson, W. F., and G. Csanady, 1971: The effects of atmospheric conditions on plume rise. *J. Fluid Mech.*, **47**, 33–50.
- Stommel, H., 1951: Entrainment of air into a cumulus cloud, II. *J. Meteor.*, **8**, 127–129.
- Turner, D. B., 1969: *Workbook of Atmospheric Dispersion Estimates*. U.S. Environmental Protection Agency, OAP AP-26, 84 pp.
- Weinstein, A. I., 1972: Ice phase seeding potential for cumulus cloud modification in the western United States. *J. Appl. Meteor.*, **11**, 202–210.
- Wisner, C. E., H. D. Orville and C. G. Myers, 1972: A numerical model of a hail-bearing cloud. *J. Atmos. Sci.*, **29**, 1160–1181.